Measurement of Nonplanar Dielectric Samples Using an Open Resonator

W. F. P. CHAN AND BARRY CHAMBERS

Abstract—Conventional microwave methods for measuring permittivity often utilize samples in flat sheet form. In practice, however, it is sometimes desirable to measure samples having curved surfaces, for example, parts of lenses or small radomes. This paper describes an open resonator technique for achieving this and compares measurements made at 11.6 GHz on samples of polymethyl methacrylate in both curved and flat sheet form.

I. Introduction

A PROBLEM OF continuing interest is that of measuring the spatial variations in dielectric constant and loss tangent within a dielectric object of complex shape, such as a lens or a missile radome, especially at high temperatures. Most techniques employed previously for this type of measurement have been destructive in that samples of material have had to be removed from the object under investigation and carefully machined before being measured in a waveguide system. The samples thus measured are flat, but for a nondestructive measurement, *in situ* samples are necessarily curved and thus an open resonator technique, rather than a waveguide one, appears to be more suitable.

The open resonator has been shown previously to provide an accurate and convenient tool for the measurement of the complex permittivity of dielectric materials in flat sheet form [1]–[6], and Cullen and Yu [1] were the first to use Gaussian beam theory to analyze such a system. Normally, measurements are made with the sample located centrally within the resonator so as to match the wavefronts approximately to the sample surfaces. Perturbation theory is then used to compensate for the deviation of the sample geometry from the ideal biconvex geometry required. Since this deviation is usually small, experimental errors of less than 1 percent for relative permittivity and 10 percent for loss tangent are typical of those which have been reported for various flat samples.

In an earlier paper [7], we presented the results of a study into the measurement of biconcave dielectric samples using an open resonator and examined the applicability of the perturbation theory in these cases. More recently, by using arguments similar to those employed by Cullen and Yu [1], we have developed a new technique for the measurement of convex–concave dielectric samples, and preliminary results were reported in [8]. In the new measurement configuration, convex–concave samples are measured at off-center positions inside the open resonator where the wavefronts are curved and therefore similar in form to the sample surfaces. By assuming that the latter are coincident with the wavefronts, the field equations applied at the air–dielectric interfaces can be simplified. At resonance, the wave impedances on either side of the two curved air–dielectric interfaces can be equated and two transcendental equations, one for each air–dielectric interface, can be obtained from which to calculate the relative permittivity. When this has been determined, the loss tangent can be obtained by calculating the difference in energy losses between the unloaded and loaded resonators.

A comprehensive experimental study of the new measurement configuration has been completed and results for polymethyl methacrylate (perspex) samples measured at 11.6 GHz are reported, together with a discussion of experimental errors.

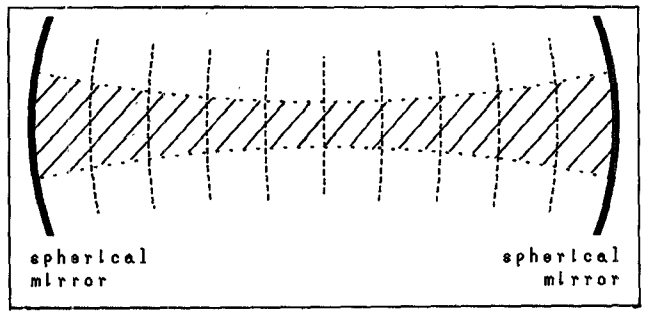

Fig. 1. An open resonator formed by a pair of spherical mirrors. ----- radii of curvature of the wavefronts. ///// shape of the Gaussian beam.

II. Theory

An open resonator formed by a pair of identical spherical mirrors, as shown in Fig. 1, supports a complete and orthogonal set of resonance modes. In practice, however, due to the diffraction losses caused by the limited mirror aperture, only the fundamental and a few low-loss higher order modes actually exist. In the analysis which follows, only the fundamental mode of resonance is considered. This mode can be described in terms of a Gaussian beam which propagates between the mirrors to form a standing wave pattern. The beam has its minimum width at the

Manuscript received April 6, 1987; revised August 6, 1987.

The authors are with the Department of Electronic and Electrical Engineering, University of Sheffield, Sheffield S1 3JD England.

IEEE Log Number 8717108.

0018-9480/87/1200-1429$01.00 ©1987 IEEE

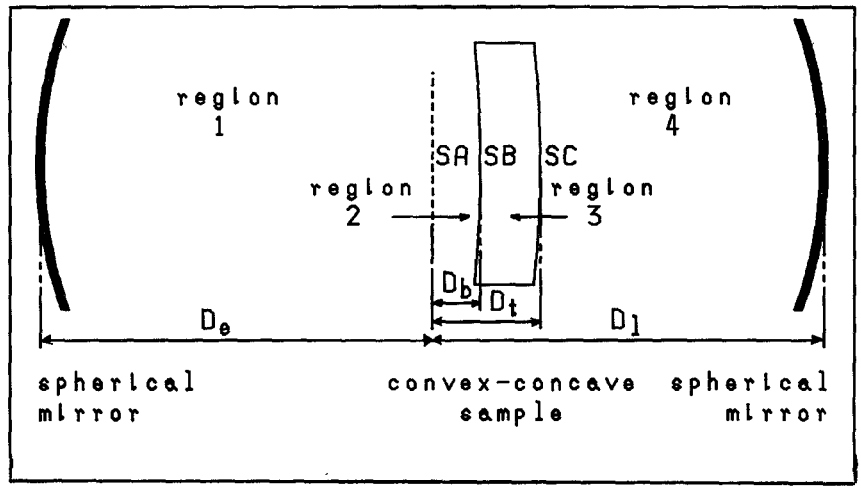

Fig. 2. New measurement configuration.

center of the resonator and expands as it propagates away from the center. The radius of curvature of the wavefronts decreases from infinity at the center of the resonator to that of the mirrors at their surfaces. Following Kogelnik and Li [9], the electromagnetic field of a Gaussian beam is given by the following equations:

$$E_x = \frac{w_0}{w}\exp\left(\frac{-r^2}{w^2}\right)\exp\left(kz - \Phi + \frac{kr^2}{2R}\right) \quad (1)$$

$$H_y = \frac{w_0}{Z_0 w}\exp\left(\frac{-r^2}{w^2}\right)\exp\left(kz - \Phi + \frac{kr^2}{2R}\right) \quad (2)$$

where w_0 is the minimum width of the beam, k is the free-space phase constant, r is the radius, Z_0 is the free-space wave impedance. The beamwidth w, radius of curvature of the wavefront R, and the extra phase shift Φ are defined by

$$w^2(z) = w_0^2\left[1 + \left(2z/kw_0^2\right)^2\right]$$

$$R(z) = z\left[1 + \left(kw_0^2/2z\right)^2\right]$$

$$\Phi(z) = \tan^{-1}\left(2z/kw_0^2\right). \quad (3)$$

As shown here, the electromagnetic field is assumed to be linearly polarized. This assumption holds as long as $(kw_0)^{-2} \ll 1$.

Since the radius of curvature of the wavefronts varies with position along the longitudinal axis of the resonator, accurate measurements on convex–concave samples should be possible by placing them nearer to one of the mirrors, where the radii of curvature of the sample surfaces are similar to those of the wavefronts. When, for example, such a sample is located nearer to the right-hand mirror, as shown in Fig. 2, the system can be envisaged as being comprised of four regions, separated by three constant-phase surfaces. These are the plane surface SA, where the beamwidth is a minimum, and the two air–dielectric interfaces SB and SC. In region 1, the field can be written as

$$E_{x1} = \frac{A_1 w_{01}}{w_1}\exp\left(\frac{-r^2}{w_1^2}\right)\sin\left(kz - \Phi_1 + \frac{kr^2}{2R_1} + \alpha\right) \quad (4)$$

$$H_{y1} = \frac{jA_1 w_{01}}{Z_0 w_1}\exp\left(\frac{-r^2}{w_1^2}\right)\cos\left(kz - \Phi_1 + \frac{kr^2}{2R_1} + \alpha\right) \quad (5)$$

where the beam has its minimum width of w_{01} at $z = 0$, A_1 is an amplitude factor, and w_1, R_1, and Φ_1 are defined by

$$w_1^2(z) = w_{01}^2\left[1 + \left(2z/kw_{01}^2\right)^2\right]$$

$$R_1(z) = z\left[1 + \left(kw_{01}^2/2z\right)^2\right]$$

$$\Phi_1(z) = \tan^{-1}\left(2z/kw_{01}^2\right). \quad (6)$$

α is a constant which can be found by applying suitable boundary condition at the left-hand mirror surface. Here the tangential electric field is zero. From (4),

$$\alpha = +kD_e - \Phi_1(D_e) \quad (7)$$

and (4) and (5) become

$$E_{x1} = \frac{A_1 w_{01}}{w_1}\exp\left(\frac{-r^2}{w_1^2}\right) \cdot \sin\left(kz - \Phi_1 + \frac{kr^2}{2R_1} + kD_e - \Phi_1(D_e)\right) \quad (8)$$

$$H_{y1} = \frac{jA_1 w_{01}}{Z_0 w_1}\exp\left(\frac{-r^2}{w_1^2}\right) \cdot \cos\left(kz - \Phi_1 + \frac{kr^2}{2R_1} + kD_e - \Phi_1(D_e)\right). \quad (9)$$

As regions 1 and 2 are separated by a virtual surface SA, the fields in each region can be expressed in a similar form. The reason for separating the two regions becomes obvious if a flat mirror is positioned at SA to replace the left-hand spherical mirror, since this results in the hemispherical open resonator, a configuration which is frequently used for dielectric measurements. Hence,

measurement of convex–concave samples can also be made using a hemispherical open resonator and the theoretical analysis of such a system will be slightly simpler than the present one. In our analysis, however, regions 1 and 2 will remain separated and the field in region 2 is therefore given by (6), (8), and (9), where the subscript 1's are replaced by 2's. In region 3, the beam is treated as a portion of a virtual beam which has its minimum width w_{03} at $z = z_3$. The field can therefore be written as

$$E_{x3} = \frac{A_3 w_{03}}{w_3} \exp\left(\frac{-r^2}{w_3^2}\right) \sin\left(nkz - \Phi_3 + \frac{nkr^2}{2R_3} + \beta\right) \quad (10)$$

$$H_{y3} = \frac{jA_3 w_{03}}{Z_1 w_3} \exp\left(\frac{-r^2}{w_3^2}\right) \cos\left(nkz - \Phi_3 + \frac{nkr^2}{2R_3} + \beta\right) \quad (11)$$

where n is the refractive index of the dielectric, Z_1 is the wave impedance of the dielectric, and β is a constant determined by the sample position. The quantities w_3, R_3, and Φ_3 are defined by

$$\begin{aligned} w_3^2(z) &= w_{03}^2\left\{1 + \left[2(z - z_3)/nkw_{03}^2\right]^2\right\} \\ R_3(z) &= (z - z_3)\left\{1 + \left[nkw_{03}^2/2(z - z_3)\right]^2\right\} \\ \Phi_3(z) &= \tan^{-1}\left[2(z - z_3)/nkw_{03}^2\right]. \end{aligned} \quad (12)$$

In region 4, the beam is again treated as a portion of another virtual beam which has its minimum width w_{04} at $z = z_4$, and the field in this region can therefore be written as

$$E_{x4} = \frac{A_4 w_{04}}{w_4} \exp\left(\frac{-r^2}{w_4^2}\right) \sin\left(kz - \Phi_4 + \frac{kr^2}{2R_4} + \gamma\right) \quad (13)$$

$$H_{y4} = \frac{jA_4 w_{04}}{Z_0 w_4} \exp\left(\frac{-r^2}{w_4^2}\right) \cos\left(kz - \Phi_4 + \frac{kr^2}{2R_4} + \gamma\right) \quad (14)$$

where w_4, R_4, and Φ_4 are defined by

$$\begin{aligned} w_4^2(z) &= w_{04}^2\left\{1 + \left[2(z - z_4)/kw_{04}^2\right]^2\right\} \\ R_4(z) &= (z - z_4)\left\{1 + \left[kw_{04}^2/2(z - z_4)\right]^2\right\} \\ \Phi_4(z) &= \tan^{-1}\left[2(z - z_4)/kw_{04}^2\right]. \end{aligned} \quad (15)$$

γ is a constant which can be found by applying the boundary condition at the right-hand mirror surface. Thus

$$\gamma = -kD_l + \Phi_4(D_l) \quad (16)$$

and (13) and (14) become

$$E_{x4} = \frac{A_4 w_{04}}{w_4} \exp\left(\frac{-r^2}{w_4^2}\right) \cdot \sin\left(kz - \Phi_4 + \frac{kr^2}{2R_4} - kD_l + \Phi_4(D_l)\right) \quad (17)$$

$$H_{y4} = \frac{jA_4 w_{04}}{Z_0 w_4} \exp\left(\frac{-r^2}{w_4^2}\right) \cdot \cos\left(kz - \Phi_4 + \frac{kr^2}{2R_4} - kD_l + \Phi_4(D_l)\right). \quad (18)$$

Assuming the air–dielectric interfaces are coincident with the wavefronts, then the wave impedances at these surfaces can be matched. Firstly, the width and the radius of curvature of the beam have to be identical on both sides of the air–dielectric interfaces. Therefore, at SB,

$$\begin{aligned} w_2(D_b) &= w_3(D_b) \\ R_2(D_b) &= R_3(D_b) \end{aligned} \quad (19)$$

whereas at SC,

$$\begin{aligned} w_3(D_t) &= w_4(D_t) \\ R_3(D_t) &= R_4(D_t). \end{aligned} \quad (20)$$

When the air–dielectric interfaces are coincident with the wavefronts, the field equations applied at these interfaces are simplified as the r-dependent terms can be ignored. The wave impedances Z_{bl} and Z_{br}, looking to the left and right of interface SB, can be written as

$$Z_{bl} = -jZ_0 \tan\left(kD_b - \Phi_2(D_b) + kD_e - \Phi_2(D_e)\right) \quad (21)$$

$$Z_{br} = -jZ_1 \tan\left(nkD_b - \Phi_3(D_b) + \beta\right) \quad (22)$$

whereas at SC, the corresponding wave impedances Z_{cl} and Z_{cr} are

$$Z_{cl} = -jZ_1 \tan\left(nkD_t - \Phi_3(D_t) + \beta\right) \quad (23)$$

$$Z_{cr} = -jZ_0 \tan\left(kD_t - \Phi_4(D_t) - kD_l + \Phi_4(D_l)\right). \quad (24)$$

At resonance, the wave impedances on both sides of the two curved air–dielectric interfaces should be equal. Hence at SB, from (21) and (22),

$$jZ_0 \tan\left(kD_b - \Phi_2(D_b) + kD_e - \Phi_2(D_e)\right) = jZ_1 \tan\left(nkD_b - \Phi_3(D_b) + \beta\right) \quad (25)$$

$$\tan\left(kD_b - \Phi_2(D_b) + kD_e - \Phi_2(D_e)\right) = (1/n)\tan\left(nkD_b - \Phi_3(D_b) + \beta\right) \quad (26)$$

whereas at SC, from (23) and (24),

$$jZ_1 \tan\left(nkD_t - \Phi_3(D_t) + \beta\right) = jZ_0 \tan\left(kD_t - \Phi_4(D_t) - kD_l + \Phi_4(D_l)\right) \quad (27)$$

$$(1/n)\tan\left(nkD_t - \Phi_3(D_t) + \beta\right) = \tan\left(kD_t - \Phi_4(D_t) - kD_l + \Phi_4(D_l)\right). \quad (28)$$

When the relative permittivity ϵ_r has been determined by $\epsilon_r = n^2$, the loss tangent of the sample can be obtained by calculating the difference in energy losses between the unloaded and the loaded resonators. The loss tangent is therefore given by

$$\tan\delta = \left(\frac{1}{Q_l} - \frac{1}{Q_e}\right) \cdot \left(\frac{\int_{v_1} |E_{x1}|^2\, dv + \int_{v_2} |E_{x2}|^2\, dv + \epsilon_r \int_{v_3} |E_{x3}|^2\, dv + \int_{v_4} |E_{x4}|^2\, dv}{\epsilon_r \int_{v_3} |E_{x3}|^2\, dv}\right) \quad (29)$$

where v_1, v_2, v_3, and v_4 are the volumes of the four corresponding regions and Q_e and Q_l are the unloaded and loaded Q factors, respectively.

When the radii of curvature of the sample surfaces are different from those of the wavefronts, exact matching of the wave impedances at the air–dielectric interfaces is impossible unless higher order transverse modes are also taken into account. However, small deviations of sample geometry from the ideal can be compensated for by using perturbation theory [1].

III. Experimental Study

As a test of the new theory, measurements were made at 11.6 GHz on polymethyl methacrylate disks having one convex and one concave surface using an open resonator with mirrors whose radius of curvature was 330 mm. The experimental setup is shown in Fig. 3. In all, eight samples with different radii of curvature were measured at several different positions inside the resonator where the radii of curvature of the samples were similar to the corresponding wavefronts.

When a sample is placed inside an open resonator, the system can be retuned by changing the resonant frequency. This involves adjusting the sample to be perpendicular to and aligned with the longitudinal axis of the resonator. In our measurements, a specially designed sample holder was used to provide the necessary adjustments. The changes in resonant frequency and Q factor between the unloaded and loaded resonators were measured and related to the relative permittivity and loss tangent using the theory discussed above.

The results are shown in Table I, together with the corresponding results for the same material measured in flat sheet form, using the same system. As can be seen, the results for the two cases appear consistent and are in good agreement. The slight differences between the results for samples C1–C5 and C6–C8 is attributed to the fact that each group of samples was cut from different sheets of material. Apart from these slight differences, experimental errors appear to be due mainly to uncertainties in the measurement of sample position, sample geometry, resonant frequency, and Q factor.

When making measurements, the position of the sample inside the resonator needs to be known accurately, and this has proved to be a source of difficulty. However, by adjusting the position of the sample to produce either a maximum or a minimum shift in resonant frequency, only a rough estimation of the sample position is required. The actual position can then be calculated using a technique which seeks the optimum value of the relative permittivity, expressed as either a maximum or a minimum calculated value, as the position of the sample is allowed to vary slightly about the estimated value. By using this technique, the uncertainty in sample position was kept less than ± 0.5 mm, and this was calculated to give variations in relative permittivity and loss tangent for all samples of less than 1.5 percent and 15 percent, respectively. Variations in the complex permittivity for sample C8 are shown in Table II. As can be seen, variations are larger when samples were measured in low field regions where the relative field intensity at the air–dielectric interfaces was high. In our measurements, the angular position of the sample could be adjusted to better than $\pm 1°$ and the changes in resonant frequency and Q factor due to the resulting slight variations in sample aspect were found to be negligible.

Since most of the energy of the Gaussian beam is concentrated near its longitudinal axis, as long as the sample is large enough to intercept the latter, the transverse dimensions of the sample are not critical. However, the thickness of the samples still needs to be known

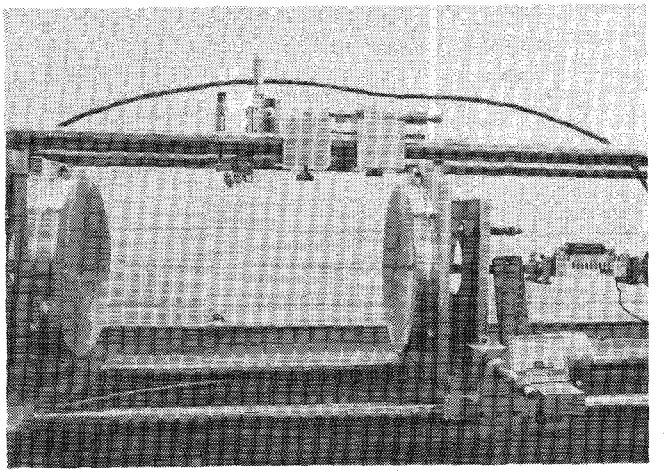

Fig. 3. Experimental setup.

TABLE I
Measurement Results for Flat and Convex–Concave Samples

(a) results for convex-concave samples.

sample number	radius of curvature of concave surface	radius of curvature of convex surface	measured in high field region: relative permittivity	measured in high field region: loss tangent	measured in low field region: relative permittivity	measured in low field region: loss tangent
C1	5.603m	3.787m	2.628	0.0070	2.613	0.0066
C2	2.497m	2.062m	2.627	0.0069	2.602	0.0066
C3	1.402m	1.257m	2.627	0.0069	2.594	0.0065
C4	0.874m	0.823m	2.629	0.0069	2.623	0.0065
C5	0.648m	0.625m	2.631	0.0070	2.632	0.0064
variations in			0.2%	1%	1.5%	3%
a) relative permittivity			----------	1.5%	----------	
b) loss tangent				----------	9%	----------
C6	0.488m	0.478m	2.590	0.0043	2.617	0.0050
C7	0.386m	0.384m	2.582	0.0041	2.621	0.0050
C8	0.330m	0.330m	2.581	0.0043	2.621	0.0057
variations in			0.3%	5%	0.2%	13%
a) relative permittivity			----------	1.5%	----------	
b) loss tangent				----------	34%	----------

(b) results for flat samples.

sample number	thickness of sample	measured in high field region: relative permittivity	measured in high field region: loss tangent	measured in low field region: relative permittivity	measured in low field region: loss tangent
F1	3.01mm	2.611	0.0059	2.621	0.0062
F2	4.01mm	2.620	0.0060	2.617	0.0064
F3	5.01mm	2.619	0.0063	2.621	0.0065
F4	5.97mm	2.616	0.0060	2.619	0.0063
F5	6.98mm	2.617	0.0061	2.613	0.0059
F6	7.99mm	2.618	0.0061	2.610	0.0061
variations in		0.3%	7%	0.4%	10%
a) relative permittivity		----------	0.4%	----------	
b) loss tangent			----------	10%	----------

Frequency: 11.59 GHz.
Material: polymethyl methacrylate (Perspex).
Radius of curvature of mirrors: 330 mm.

TABLE II
VARIATIONS IN RELATIVE PERMITTIVITY AND LOSS TANGENT DUE TO UNCERTAINTY IN SAMPLE POSITION

sample number	sample position	measured in high field region: relative permittivity	measured in high field region: loss tangent	measured in low field region: relative permittivity	measured in low field region: loss tangent
C8	-0.5mm	2.615	0.0041	2.596	0.0065
C8	original value	2.590	0.0044	2.624	0.0060
C8	+0.5mm	2.616	0.0047	2.596	0.0057
variations		1.0%	15%	1.2%	14%

TABLE III
VARIATIONS IN RELATIVE PERMITTIVITY AND LOSS TANGENT DUE TO UNCERTAINTY IN SAMPLE THICKNESS

sample number	sample thickness	measured in high field region: relative permittivity	measured in high field region: loss tangent	measured in low field region: relative permittivity	measured in low field region: loss tangent
C8	-0.03mm	2.592	0.0044	2.642	0.0060
C8	5.87mm	2.590	0.0044	2.624	0.0060
C8	+0.03mm	2.587	0.0044	2.605	0.0060
variations		0.2%	0%	1.4%	0%

accurately. In our repeated thickness measurements (thickness at the center of the samples), due to difficulty in alignment between the sample and the micrometer, a measurement accuracy of ± 0.03 mm was observed. By changing the assumed thickness in our analysis, variations in relative permittivity were less than 0.2 percent and 1.5 percent when samples were measured in high and low field regions of the resonator, respectively. However, variations in loss tangent for samples measured in both high and low field regions were small. Table III shows the variations in relative permittivity and loss tangent due to assumed variations in thickness.

Perturbation theory compensation has been applied to the results to account for the deviations from the ideal geometry of the convex–concave samples, but since these were designed to match approximately with the wavefronts, the compensation is small. When, however, the sample geometry is very different from the ideal, the errors are expected to be large and dominated by those introduced by the use of perturbation theory. These errors can be minimized, as reported in [7], by locating the sample in a high field region of the resonator standing wave pattern while leaving the air–dielectric interfaces in relatively low field regions. Hence refraction of the electric field can be minimized together with the errors. Alternatively, by using mirrors whose radii of curvature are similar to those of the sample surfaces, wavefronts with similar radii of curvature can be produced to match the sample geometry.

Errors in relative permittivity and loss tangent arising from uncertainties in the measured resonant frequency and Q factor are typically within 1 percent and 5 percent, respectively. After taking the above-mentioned factors into account, the uncertainties in the relative permittivity and loss tangent are expected to be within 3 percent and 20 percent, respectively. As can be seen from Table I, the results obtained for samples measured in similar field intensity regions appear to be consistent, but a relatively large difference occurs between those measured in high and low field regions. When the results for samples measured in both regions are combined together, experimental errors are 1.5 percent and 35 percent for relative permittivity and loss tangent, respectively. As the errors appear to increase when the radius of curvature is small, this is thought to be due to incomplete field matching at the air–dielectric interfaces, since the width of the beam has only been matched at the center point and not across the whole interface.

IV. DISCUSSION

The new measurement technique has certain advantages over that employed for flat sheet samples. As the sample is not required to be positioned at a particular point within the resonator, the resonant frequency can be varied by moving the sample along the longitudinal axis. Measurement of the complex permittivity over a range of frequencies should therefore be possible although the frequency range may not be extensive. However, by measuring the sample at different positions along the longitudinal axis using several different axial order modes, the frequency range can be greatly extended.

Since the new technique is capable of measuring a sample positioned close to one of the mirrors, a symmetrical resonator is not always necessary. This is a particularly useful feature when access around the object under investigation is limited. Thus a nonsymmetrical resonator formed from a flat mirror and a concave mirror, or an even more compact configuration of a convex mirror and a concave mirror could be used.

The new technique does have one disadvantage, however. Normally, for the measurement of flat samples, only the thickness of the latter need be known accurately. When using the new configuration, however, a fuller description of the sample geometry is required; thus additional errors can arise.

V. CONCLUSIONS

A new technique for the measurement of convex–concave dielectric samples using an open resonator has been developed which involves positioning a sample such that its surfaces coincide approximately with particular wavefronts within the resonator. Measurements have been made at 11.6 GHz on polymethyl methacrylate disk samples with radii of curvature as small as 330 mm. The results obtained appear consistent and are in good agreement with those for the same material measured in flat sheet form.

When the sample surfaces are approximately coincident with the wavefronts, experimental errors are due mainly to uncertainties in the measurement of sample geometry, sample position, resonant frequency, and Q factor. Experimental errors within 1.5 percent for relative permittivity and 35 percent for loss tangent have been obtained. These are thought in part to be due to imperfect field matching at the air–dielectric interfaces.

ACKNOWLEDGMENT

The authors would like to thank Dr. A. C. Lynch of the University College, London, for his valuable discussions about the new technique.

REFERENCES

[1] A. L. Cullen and P. K. Yu, "The accurate measurement of permittivity by means of an open resonator," *Proc Royal Soc. London, Ser. A.*, vol. 325, pp. 493–509, 1971.

[2] R. J. Cook, R. G. Jones, and C. B. Rosenberg, "Comparison of cavity and open resonator measurement of permittivity and loss angle at 35 GHz," *IEEE Trans. Instrum. Meas.*, vol. IM-23, pp. 438–442, 1974.

[3] R. J. Cook and R. G. Jones, "Correction to open-resonator permittivity and loss measurements," *Electron Lett.*, vol. 12, pp. 1–2, 1976.

[4] A. L. Cullen and P. K. Yu, "Measurement of permittivity by means of an open resonator, I. Theoretical." *Proc Royal Soc. London, Ser. A.*, vol. 380, pp. 49–71, 1982.

[5] A. C. Lynch, "Measurement of permittivity by means of an open resonator. II. Experimental." *Proc Royal Soc. London, Ser. A.*, vol. 380, pp. 73–76, 1982.

[6] A. C. Lynch, "Measurement of permittivity using an open resonator," *Proc. Inst. Elec. Eng.*, pt. A, vol. 130, no. 7, pp. 365–368, 1983.

[7] W. F. P. Chan and B. Chambers, "Measurement of the complex permittivity of curved dielectric radome specimens using an open resonator," in *Proc. 16th European Microwave Conf.*, (Dublin, Ireland), Sept. 1986, pp. 796–801.

[8] W. F. P. Chan and B. Chambers, "A new technique for the measurement of the complex permittivity of curved dielectric specimens using an open resonator," in *Proc. 5th Int. Conf. Antennas Propagat.*, (York, UK), Apr. 1987.

[9] H. Kogelnik and Li, T. "Laser beams and resonators," *Proc IEEE*, vol. 54, pp. 1312–1329, 1966.

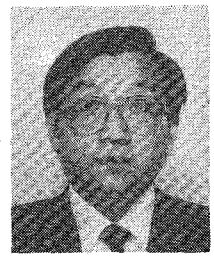

W. F. P. Chan was born in Hong Kong. He graduated from the Department of Electronic and Electrical Engineering at the University of Sheffield, U.K., in 1983. He is currently reading for the Ph.D. degree with the same department.

✠

Barry Chambers received the Ph.D. degree in electronic engineering from the University of Sheffield, U.K., in 1968.

From then until 1971, he was a Teaching Fellow and then an Assistant Professor with the Department of Electrical Engineering at the University of British Columbia in Vancouver, Canada. During this period he worked on surface waveguides and resonators and ferrite phase shifters. In 1971, he rejoined the University of Sheffield, where he is now a Senior Lecturer in the Antennas and Propagation Group in the Department of Electronic and Electrical Engineering. His current research interests are in the fields of electromagnetic wave propagation and scattering, radomes, and stealth technology.

Dr. Chambers is a member of the Institution of Electrical Engineers and a Chartered Engineer.